FULL PAPER

Bingel-Hirsch Addition of Diethyl Bromomalonate to Ion-Encapsulated Fullerene M@C_{60} (M = ∅, Li^+, Na^+, K^+, Mg^{+2}, Ca^{+2}, and Cl^-)

Pau Besalú-Sala, Josep M. Luis* and Miquel Solà*

[a] P. Besalú-Sala, Dr. J. M. Luis, Prof. Dr. M. Solà
Institut de Química Computacional i Catàlisi (IQCC) and Departament de Química
Universitat de Girona
C/ Maria Aurèlia Capmany, 69, 17003, Girona, Catalonia (Spain)
E-mail: josepm.luis@udg.edu, miquel.sola@udg.edu

Supporting information for this article is given via a link at the end of the document.

Abstract: In the last 30 years, fullerene-based materials have become popular building blocks for devices with a broad range of applications. Among fullerene derivatives, endohedral metallofullerenes (EMFs, M@C_x) have been widely studied due to their unique properties and reactivity. For real applications, fullerenes and EMFs must be exohedrally functionalized. It has been shown that encapsulated metal cations facilitate the Diels-Alder reaction in fullerenes. Herein, we quantum mechanically explore the Bingel-Hirsch (BH) addition of ethyl bromomalonate over a series of ion-encapsulated M@C_{60} (M = ∅, Li^+, Na^+, K^+, Mg^{+2}, Ca^{+2}, and Cl^-) to analyze the effect of these ions on the BH addition. Our results show that the incarcerated ion has very important effect on the kinetics and thermodynamics of this reaction. Among the systems studied, K^+@C_{60} is the one that leads to the fastest BH reaction, whereas the slowest reaction is given by Cl^-@C_{60}.

Introduction

One of the most interesting properties that fullerenes bear is their ability to encapsulate atoms, small molecules, and metal clusters. In particular, I_h-C_{60} (hereafter C_{60}) is able to encapsulate small atoms such as He or Ne; ions like Li^+ or even small molecules such as H_2, HF, H_2O or even CH_4.[1] If the encapsulated species is a metallic atom or a metal cluster, the resultant species is called endohedral metallofullerene (EMF).[2] Fullerenes and EMFs have a large number of promising applications in biosciences, radiotherapy, molecular switching devices, magnetic materials, and photovoltaics among others.[3]

To turn the fullerenes and EMFs into building blocks for real applications taking advantage of such interesting properties and abilities, they must be exohedrally functionalized to enhance their solubility or to furnish them with addends that improve their intrinsic properties.[2e, 4] First C_{60} functionalization did not appeared until 1991, when Wudl et al. produced fulleroids by incremental addition of a divalent carbon to C_{60}.[5] From that point on, more and more synthetic strategies have been developed by several research groups, reaching a point that, in practice, almost every functional group can be added to C_{60} through nucleophilic and electrophilic additions, pericyclic reactions, hydrogenations, oxidations, hydroxylations, or radical additions among others.[4d, 6]

Same scenario holds for C_{60}-based EMFs, which are commonly functionalized through Diels–Alder,[7] 1,3-dipolar (or Prato),[6a, 8] and Bingel–Hirsch (BH)[9] cycloadditions. The BH addition is a nucleophilic [2+1] cycloaddition reaction between a fullerene and a bromomalonate in the presence of a strong base such as 1,8-diazabicycloundec-7-ene (DBU) or sodium hydride to produce the cyclopropanated BH product. Since C_{60} obeys the so-called isolated pentagon rule (IPR),[10] there are only two different bonds in C_{60} and C_{60}-based EMFs, namely, the [5,6] and the [6,6] bonds (see Scheme 1). In the first step of the BH reaction mechanism, the base abstracts the acidic proton of the diethyl bromomalonate to generate the corresponding enolate. Then, the enolate nucleophilically attacks the fullerene generating a new carbanion with charge delocalized over the fullerene cage. In the final step, a S_N2-type nucleophilic substitution reaction occurs when the carbanion, formally in an adjacent carbon to the one bonded to the bromomalonate, attacks the α-carbon of the enolate causing an intramolecular three-membered ring closure and the release of the bromide anion.

The first BH reaction on an EMFs was performed by Alfrod et al.[11] on Gd@C_{60} to produce the highly soluble Gd@C_{60}[$C(COOH)_2$]$_{10}$ species. In 2005, Echegoyen et al.[12] reported the first BH reaction on I_h-C_{80}-based EMFs. They were able to react Y_3N@I_h-C_{80} and Er_3N@I_h-C_{80} with diethyl bromomalonate under mild conditions but failed to functionalize Sc_3N@I_h-C_{80} and Lu_3N@I_h-C_{80}. Very recently, the same group showed that the oxidized forms of these two EMFs successfully underwent BH reaction generating [5,6]- and [6,6]-open adducts.[13]

Scheme 1 illustrates the mechanism of the BH reaction in a model M@C_{60} EMF, in which we have introduced the nomenclature used throughout the manuscript. Accordingly, for each species with an endohedral ion M (M = Ø, Li^+, Na^+, K^+, Mg^{+2}, Ca^{+2}, and Cl^-, where Ø@C_{60} stands for C_{60} without any endohedral metal), the reaction mechanism starts with the formation of the the reactant complex (**M-R**) from reactants at infinite distance (**M-Rinf**). Then, the initial nucleophilic attack (**M-TS1**) of the bromomalonate to one of the 60 equivalent carbons (C^1, Scheme 1) leads to the formation of a singly bonded derivative, which is labelled as the intermediate structure (**M-I**). Subsequently, a second transition state structure (**M-TS2**) corresponding to the S_N2 reaction is reached. **M-TS2**

leads to the three-membered-ring closure, which is carried out by one of the three adjacent carbons to C^1. If carbon C^2 (see Scheme 1, inset) acts as the nucleophile, the [6,6] cycloaddition is obtained. Otherwise, if the nucleophilic attack is carried out by C^3 or C^4, the [5,6] product is obtained. We shall see in subsequent section of the manuscript that this is not going to occur in practice due to their higher associated Gibbs energy barriers. In fact, the [5,6] addition in BH reactions has been reported only for few EMFs,[13-14] although in some cases, the [6,6] adducts could be further converted to [5,6] products by heating.[15] The functionalized EMF product can be considered a closed-cage methanofullerene **M-P** or an open-cage fulleroid **M-P'** depending on C^1-C^2 distance. Finally, the products with the NaBr molecule at infinite distance will be also computed, and labeled as **M-Pinf/M-P'inf**.

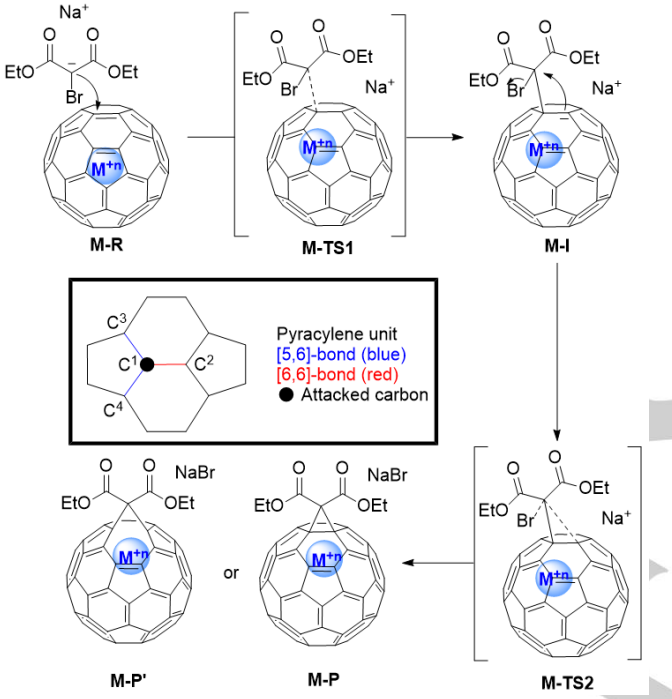

Scheme 1. Lewis structure representation of the Bingel-Hirsch reaction over a general M@C60 EMF. Inset: top view of a pyracylene unit indicating the attacked carbon in **M-TS1** and the different [5,6]- (blue) and [6,6]- (red) bonds.

Recently, ion-encapsulated fullerenes, *i.e.* fullerenes having an endohedral ion, have emerged as a new family of endohedral fullerenes.[1e, 16] In the particular case of the Diels-Alder (DA) addition, a significant enhancement of the reaction rate was found for those systems having an endohedral cation.[17] Thus, the DA reactions between cyclopentadiene and $Li^+@C_{60}$ were reported to be significantly faster than the analogous processes involving the parent C_{60} fullerene. Theoretically, it was found that increasing the charge of the encapsulated cation (for instance, in $Be^{2+}@C_{60}$ or $Al^{3+}@C_{60}$) makes the DA even faster.[18] The reason for the observed enhanced in the rate constant of DA reactivity of cation-encapsulated fullerenes lies mainly in a much stronger HOMO(diene)→LUMO(C_{60}) interaction because of the stabilization of the LUMO(C_{60}) due to the presence of the cation.[18]

In this manuscript, the reaction mechanism for the BH addition of diethyl bromomalonate to M@C_{60} (M = Ø, Li^+, Na^+, K^+, Mg^{+2}, Ca^{+2}, and Cl^-) is computationally explored by means of density functional theory (DFT). Our aim is to discuss and clarify the effect of the encapsulated ions in the kinetics and thermodynamics of the BH reaction. It is likely that an encapsulated cation can speed up the first attack of the BH reaction, but on the other side it may also slow down the second S_N2-type nucleophilic substitution reaction. Therefore, it is not clear whether the cation will increase or decrease the reaction rate of the BH reaction, although the reported increase of the reactivity of oxidized $Sc_3N@I_h$-C_{80} and $Lu_3N@I_h$-C_{80} EMFs as compared to their neutral counterparts seems to suggest that encapsulated cations can improve the reactivity of BH cycloadditions to fullerenes. Later on, in this article we shall reach the conclusion, which we anticipate here, that the BH reaction is accelerated by encapsulated monocations, but at variance with the DA cycloaddition, the performance deteriorates when moving from mono to dications. Additionally, in this manuscript we will discuss few technical aspects that must be taken into account for a correct modelling of the BH reactivity of EMFs, namely, the need to include the enolate's counterion and to properly treat solvent effects to avoid spurious overstabilization of some stationary points on the potential energy surface (PES).

Results and Discussion

For the C_{60} and $Li^+@C_{60}$ as a model EMF, we explored the BH additions on both the [5,6]- and [6,6]-bonds using the diethyl bromomalonate as the nucleophile. Both bonds show the same mechanism. The attack on the [6,6]-bond was kinetically favored over the [5,6]-bond by 24.4 kcal·mol^{-1} (C_{60}) and 7.7 kcal·mol^{-1} ($Li^+@C_{60}$), as can be seen in Figure 1. This result concurs with the fact that [5,6]-bond functionalization has not been experimentally observed for C_{60}.[9] As found for the DA cycloaddition, encapsulation of Li^+ in C_{60} favors both the [6,6]-

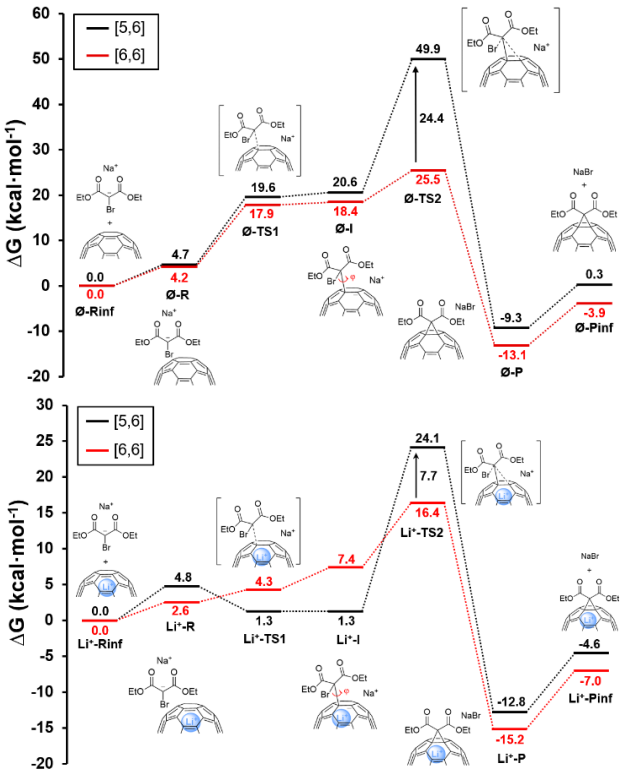

Figure 1. Reaction profiles (ΔG, kcal·mol^{-1}) for the BH addition of diethyl bromomalonate into a C_{60} fullerene (top) and $Li^+@C_{60}$ EMF (bottom) attacking at [5,6]-bond (black) and [6,6]-bond (red).

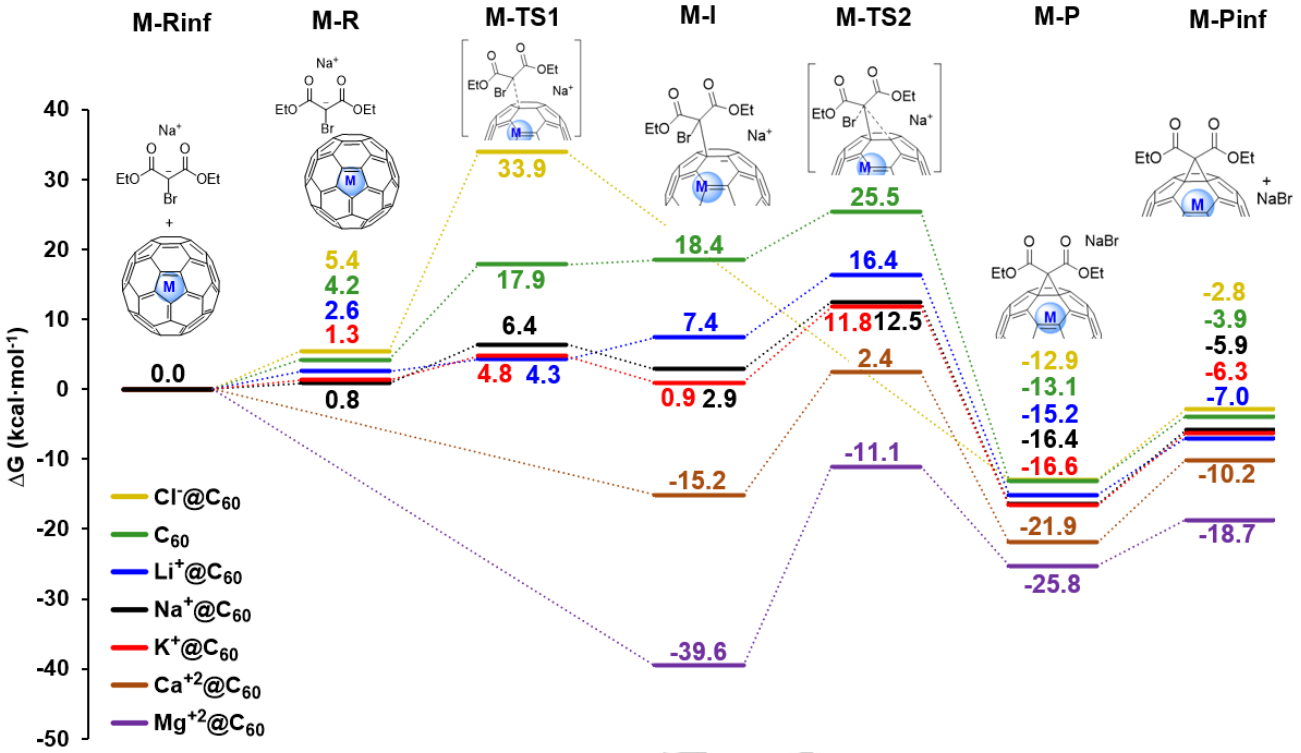

Figure 2. Reaction profiles (ΔG, kcal·mol^{-1}) for the BH addition into a [6,6]-bond of M@C_{60} (M = ∅, Li^+, Na^+, K^+, Mg^{+2}, Ca^{+2}, and Cl^-).

and the [5,6]-attacks compared with C_{60}.[18] The Gibbs energy reaction barrier of 25.5 and 16.4 kcal·mol^{-1} for the BH cycloaddition to the [6,6] bond of C_{60} and $Li^+@C_{60}$ are not far from barriers reported in previous computational studies of BH additions.[13, 19] To be consistent with results shown later on, we included the effect of the Na^+ counterion of the diethyl bromomalonate anion in the comparison of both attacks. From now on, we will focus our study on the [6,6] attack due to the higher energy barrier of the [5,6] attack in both systems, plus the fact that, to the best of our knowledge, direct [5,6] attacks have never been observed for BH additions to C_{60}.

The results obtained for the BH addition to the [6,6] bond of different M@C_{60} species studied are displayed in Figure 1. The first step of the [6,6] reaction is the approach of the reactants from infinite distance to a shorter distance forming the reactant complex (**M-R**). In this step the bromomalonate extend its arms interacting with the surface of the fullerenic cage and is placed between the carbon cage and the Na^+ counterion. This approximation of the reactants breaks the symmetry of the EMFs since the endohedral metal is no longer placed in the middle of the cage, but is displaced towards the reacting carbon, C^1. Dispersion interactions turn out to be key and must be included for the success of modelling such processes.[20]

Then, the diethyl bromomalonate anion nucleophilically attacks the fullerenic cage leading to the intermediate **M-I**, in which the diethyl bromomalonate is singly bonded to the fullerene at C^1, which hybridizes to sp^3. At this point, the negative charge is formally transferred to C^2. Except for M = ∅ and Cl^-, the Gibbs energy barrier (**M-TS1**) for this step is lower than 7 kcal·mol^{-1}. As expected, the larger the positive charge of M, the lower barrier for the nucleophilic attack. In fact, this attack has no barrier for M = Mg^{2+} and Ca^{2+}. On the contrary, $Cl^-@C_{60}$ presents the highest Gibbs energy barrier for this step, as the reaction mechanism requires the approach of two negatively charged species. Intermediate **M-I** presents a σ-bond between the bromomalonate group and the fullerenic cage, which, in principle, can rotate generating several conformations that could let to two (due to symmetry) different products. The barriers for the interconversion of the different orientational isomers of malonate are very low and accessible at room temperature.[19a, b, e] In all cases, we report the conformer that ultimately leads to the [6,6]-product, which is connected to **M-TS2** by IRC calculations.

The next step of the reaction is the formation of the 3-membered-ring. The transition state of this step (**M-TS2**) is the rate determining transition state for all the cases except for $Cl^-@C_{60}$. In **M-TS2**, the carbanion formed in C^2, nucleophilically attacks the diethyl bromomalonate in a S_N2 fashion, promoting the closure of the three-membered ring and the liberation of the bromide anion as the leaving group. The bromide is captured by the Na^+, process that has a key role in stabilizing the products of this step. In the case of the $Cl^-@C_{60}$ EMF, the S_N2 attack is so favored that occurs in a concerted manner together with the initial nucleophilic attack of diethyl bromomalonate anion. The IRC calculations show that once **M-TS1** has been surmounted, the reaction evolves directly to the final products without overcoming any other barrier (see Figs. S4 and S5 in the SI). On the contrary, doping C_{60} with cations disfavor the S_N2 reaction and, therefore, an increase of the reaction barrier is observed. As a matter of fact, taking as the reference the intermediate **I**, the Gibbs energy barriers that correspond purely to the S_N2 step for C_{60}, $Li^+@C_{60}$, $Na^+@C_{60}$, $K^+@C_{60}$, $Mg^{+2}@C_{60}$, and $Ca^{+2}@C_{60}$ are 7.1, 9.0, 9.6, 10.9, 28.5, and 17.6 kcal·mol^{-1}. The more positive the charge of the endohedral ion is, the lower the nucleophilic power of the C^2 carbon atom and the higher the energy barrier of the S_N2 step. As consequence, for the particular case of $Mg^{+2}@C_{60}$, intermediate **I** is the most stable species along the reaction coordinate since the S_N2 step is endergonic. Therefore, a singly bonded product will

be the final product for the BH cycloaddition to this EMF. Singly bonded products are also found for the BH addition to La@C_{2v}-C_{82}.[19b, 21]

For EMFs formally containing the same charge in the doping cation, the barrier decreases as the mono- or dication radii becomes bigger (descending in the periodic table). When the ionic radii is bigger, the cation is geometrically closer to the formal carbanion generated on the carbon cage in the S_N2 step, thus helping to decrease the chemical barrier (see Table S2 in the SI).

Overpassing **M-TS2**, we arrive to the product of the BH reaction, which could be a closed-cage methanofullerene (**M-P**) or an open-cage fulleroid (**M-P'**). Looking at C^1-C^2 distances and C^1-C^2-C(bromomalonate) angles for the product geometries (Table 1), we determine that in all cases we have closed-cage methanofullerene products since open-cage fulleroids show C^1-C^2 distances of about or larger than 2 Å. It is true, though, that as a general rule, the C^1-C^2 distance increases as the charge of the endohedral ion increases.

Table 1 lists the overall Gibbs energy barriers of the BH addition of ethyl bromomalonate to M@C_{60} (M = Ø, Li^+, Na^+, K^+, Mg^{+2}, Ca^{+2}, and Cl^-) EMFs. Interestingly, the highest barrier corresponds to BH cycloaddition to Cl^-@C_{60}. For this system, the initial nucleophilic attack of the bromomalonate is highly impeded by the negative charge of the EMF. Moving from M = Cl^- to M = Ø, Li^+, Na^+, and K^+, the reaction becomes more favorable, since the encapsulation of monocations favor the initial nucleophilic attack without disfavoring too much the S_N2 addition. Indeed, according to our calculations, the K^+@C_{60} is the one that has the lowest overall Gibbs energy barrier. Moving from monocations to dications, M = Mg^{+2} and Ca^{+2}, the overall barrier increases because the S_N2 reaction is disfavored by the reduction of the nucleophilicity of the fullerenic cage. Indeed, for Mg^{+2}@C_{60}, the reaction is disfavored with respect to hollow C_{60}. This is a major difference respect to DA exohedral functionalization, which has been studied by our group in previous studies.[18] In the DA cycloaddition, the larger the charge of the incarcerated cation, the faster the reaction. In the BH reaction, the first step of the reaction is favored by highly charged cations, whereas the second step of the reaction is disfavored by highly charged cations. The interplay between the energy barriers of these two steps leads to an overall optimized scenario for M = K^+.

Table 1. Global barriers ($\Delta G^‡$, kcal·mol^{-1}) and key geometrical parameters of the product of the BH addition to Cl^-@C_{60}, C_{60}, Li^+@C_{60}, Na^+@C_{60}, K^+@C_{60}, Mg^{+2}@C_{60}, and Ca^{+2}@C_{60} systems.

M	$\Delta G^‡$ (kcal·mol^{-1})	C^1-C^2 distance (Å)	C^1-C^2-C(bromomalonate) angle (degrees)
Cl^-	33.9	1.56	64.3
Ø	25.5	1.59	63.2
Li^+	16.4	1.61	64.3
Na^+	12.5	1.61	64.3
K^+	11.8	1.61	64.6
Mg^{+2}	28.5	1.73	70.8
Ca^{+2}	17.6	1.79	73.5

Let us finish by briefly mentioning two technical issues that must be taken into account for a correct modelling of the BH reactivity of EMFs, *i.e.*, the role of the counterion and solvent effects. If the modelling of the BH reaction is performed without including the counterion of the diethyl bromomalonate, spurious reaction energies for the products of the BH addition to M@C_{60} (M = Li^+, Na^+, K^+, Mg^{+2}, and Ca^{+2}) EMFs are found. This problem does not occur for C_{60} or Cl^-@C_{60}. Without including the counterion the reactants and products at infinite distance are more unstable than **M-TS2**, even by 63 kcal·mol^{-1} in the most extreme case. When the ion inside C_{60} is positively charged and the counterion is not included in the calculation, upon liberation of Br^- after **M-TS2**, Br^- anion artificially attacks one of the fullerenic carbons closest to the cyclopropane ring, which becomes close to sp^3 hybridization. In an experimental setup, entropic forces would drive solvated Br^- anion far from **M-P**. Thus, **M-P** species are not properly characterized because encapsulated cations spuriously interact electrostatically with Br^- bringing it closer to C_{60}. First attempts to solve this problem consisted on adding extra diffuse functions to Br^- with the aim of better accommodate the anionic charges. Unfortunately, this is not enough and Br^- is still heavily attracted by the endohedral metal. The problem can be solved including Na^+ in the computational simulations. Na^+ is able to catch the Br^- leaving group at the last step of the reaction and the formation of Na-Br prevents the Br^- to attack the carbon cage, recovering the appropriate exergonic product. Furthermore, another very important problem occurs if Na^+ is not included; the reactant complex **M-R** and **M-TS1** are not stable for all systems that, otherwise, present such stationary points (Li^+@C_{60}, Na^+@C_{60} and K^+@C_{60}) and the reaction evolves without overcoming any barrier to get **M-I** intermediate. Again, this problem does not affect the reaction with C_{60} and Cl^-@C_{60}. Figure 3 corresponds to the spurious reaction profile for the BH reaction of diethyl bromomalonate with K^+@C_{60} obtained without the inclusion of Na^+ counterion, showing the incorrect description of the products and the lack of **M-R** and **M-TS1** species. We refer the reader to Fig. S1 of the SI for all other profiles of the same kind.

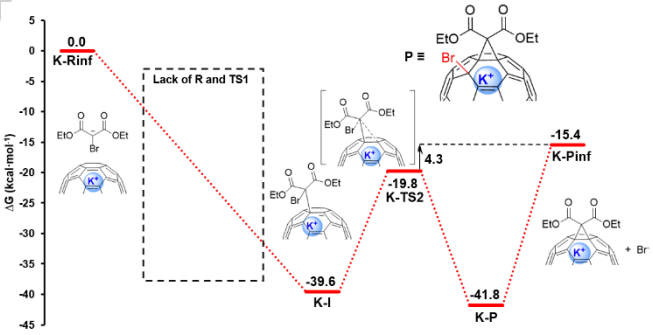

Figure 3. Reaction profile (ΔG, kcal·mol^{-1}) for the BH addition into K^+@C_{60} attacking at [6,6]-bond without the incorporation of the counterion.

It is worth noting that, for comparison purposes, Na^+ cation was added to all the systems (although for some of them was not required to obtain reasonable results) and it ended up in the same position for all the intermediates of all reactions studied (Figure 4). We observed also that Na^+ acts as a weak Lewis acid along the reaction path, staying very close to the carbonyls and thus helping to the stabilization of **M-I** and, specially, **M-TS2**. Therefore, the presence of Na^+ lowers the reaction barrier of the S_N2 process and facilitates the release of the leaving group.

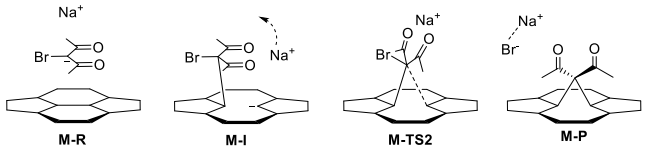

Figure 4. Position of the counterion Na^+ along the reaction path. Fullerene simplified as pyracylene unit. Ethoxy groups of the bromomalonate omitted for clarity.

Another problem that we noted when modelling the EMFs reactivity was provoked by the simulation of the solvent with the SMD model.[22] Since SMD (as many of the most used solvation models) works by placing the solute in empty spaces of the solvent polarizable continuum, sometimes the algorithm adds solvent to some places that should remain empty. This is the case for **Mg^{+2}-TS2**, for which the inside of the EMF was unrealistically filled with solvent (toluene). On the contrary, the SMD method does not place solvent inside the cage of all the other species of $Mg^{+2}@C_{60}$ reaction mechanism. This confers a spurious extra stabilization of the **Mg^{+2}-TS2** with respect to the other species and therefore, relative energies are no longer comparable, and actually can vary significantly. The way to solve this problem is discussed in the Section 2 of the ESI.

Computational Methods

All DFT calculations were performed by using the Gaussian16 program.[23] The hybrid density functional B3LYP[24] together with dispersion corrections developed by Grimme and coworkers[25] including the so-called Becke-Johnson damping[26] (D3-BJ) were used for geometrical optimizations in the gas phase, expanding the molecular orbitals (MO) over a double-ζ basis-set of Ahlrichs and coworkers, Def2SVP.[27] The use of hybrid functionals together with dispersion corrections and basis sets of similar flexibility has been proven to model properly the reactivity of fullerene and EMFs.[20, 28] All stationary points in the PES were characterized by means of analytical vibrational frequency calculations and connected through IRC calculations.[29] Single point energy corrections of reaction intermediates and transition states (TS) were performed by increasing the basis-set quality to triple-ζ Def2TZVP[30] and adding solvent corrections through the Solvation Model based on Density (SMD) model, by using toluene as solvent.[22] Therefore, the whole methodology of the study can be denoted as UB3LYP-D3BJ/Def2TZVP/SMD(Toluene)//UB3LYP-D3BJ/Def2SVP. All structures present a closed-shell singled ground state wavefunction. However, attempts to find possibly more stable *unrestricted* singlet open-shell wavefunctions were made through wavefunction stability analysis. The wavefunctions were found to be stable at the closed-shell structure for all species but one (**Mg-I**), which wavefunction and geometry was allowed to relax to its more stable unrestricted solution. For **Mg^{+2}-TS2**, SMD[22] spuriously include some polarizable continuum (toluene) potential inside the C_{60} fullerene cavity. The removal of the solvent from the interior of the C_{60} was done by adding ghost atoms inside the cavity with specific radii but without nuclear charge nor basis functions. This procedure prevents the SMD algorithm to consider solvable this empty space of the cage, and recovered a correct picture of the mechanistic profile (explained in detail in the Section 2 of the ESI).

Conclusion

In this manuscript, the reaction mechanism for the BH addition of ethyl bromomalonate to C_{60}, $Li^+@C_{60}$, $Na^+@C_{60}$, $K^+@C_{60}$, $Mg^{+2}@C_{60}$, $Ca^{+2}@C_{60}$, and $Cl^-@C_{60}$ has been elucidated by means of density functional theory calculations. Some interesting patterns regarding the BH reactivity of these EMFs have been found. The reaction goes through an initial nucleophilic attack of the bromomalonate to one of the 60 equivalent carbons that leads to the formation of a singly bonded derivative with a negative charge placed on the fullerenic cage. This attack is favored for EMFs containing positively charged cations that stabilize the negatively charged carbanion intermediate. The larger the positive charge of the encapsulated cation, the lower is the barrier of this first step. The next step corresponds to the attack of the carbanion located in the fullerene surface to the α-carbon of the enolate in a S_N2 process that causes the intramolecular three-membered ring closure that ultimately leads to the methanofullerene product and the release of the bromide anion. The higher the nucleophilic character of the carbanion, the faster the S_N2 reaction. Therefore, this attack is particularly slowed down for the EMFs containing highly positive charged cations. As a consequence of the interplay between these two steps that ideally demand opposite charges inside the EMFs to become faster, the overall Gibbs energy barrier is the lowest for C_{60} encapsulating monocations, especially for $K^+@C_{60}$, and the highest for negatively charged anions ($Cl^-@C_{60}$). Tailoring of the reaction barrier can be also achieved by varying the ionic radii of the endohedral ion, since bigger atoms are closer to the carbanion generated on **M-I** and reduce the S_N2 barrier.

Finally, we have shown that the bromomalonate's counterion should be incorporated on the calculations to achieve an appropriate modelling on the BH addition to EMFs. Otherwise, chemically nonsense structures can be achieved, especially for highly charged EMFs. Moreover, we recommend to carefully check whether solvent has been placed inside the carbon cages when modelling structures with hollow spaces.

Acknowledgements

This work was supported with funds from the Ministerio de Economía y Competitividad (MINECO) of Spain (project CTQ2017-85341-P to M.S.), the Spanish government MICINN (project PGC2018-098212-B-C22 to J.M.L), and the Generalitat de Catalunya (project 2017SGR39 to M.S. and J.M.L.). We thank the Spanish government for the predoctoral grant to P.B.-S. (FPU17/02058). We are also grateful for the computational time financed by the Consorci de Serveis Universitaris de Catalunya (CSUC).

Keywords: Endohedral metallofullerenes • solvent effects • counterion effect • Bingel cycloaddition • doped fullerenes

References

[1] a) K. Komatsu, M. Murata and Y. Murata, *Science* **2005**, *307*, 238-240; b) M. Saunders, R. J. Cross, H. A. Jiménez-Vázquez, R. Shimshi and A. Khong, *Science* **1996**, *271*, 1693-1697; c) M. Saunders, H. A. Jiménez-Vázquez, R. J. Cross, S. Mroczkowski, M. L. Gross, D. E. Giblin and R. J. Poreda, *J. Am. Chem. Soc.* **1994**, *116*, 2193-2194; d) M. Saunders, H. A. Jiménez-Vázquez, R. J. Cross and R. J. Poreda, *Science* **1993**, *259*, 1428-1430; e) S. Aoyagi, E. Nishibori, H. Sawa, K. Sugimoto, M. Takata, Y. Miyata, R. Kitaura, H. Shinohara, H. Okada, T. Sakai, Y. Ono, K. Kawachi, K. Yokoo, S. Ono, K. Omote, Y. Kasama, S. Ishikawa, T. Komuro and H. Tobita, *Nat. Chem.* **2010**, *2*, 678-683; f) K. Kurotobi and Y. Murata, *Science* **2011**, *333*, 613-616; g) A. Krachmalnicoff, R. Bounds, S. Mamone, S. Alom, M. Concistrè, B. Meier, K. Kouřil, M. E. Light, M. R. Johnson, S. Rols, A. J. Horsewill, A. Shugai, U. Nagel, T. Rõõm, M. Carravetta, M. H. Levitt and R. J. Whitby, *Nat. Chem.* **2016**, *8*, 953-957; h) S. Bloodworth, G. Sitinova, S. Alom, S. Vidal, G. R. Bacanu, S. J. Elliott, M. E. Light, J. M. Herniman, G. J. Langley, M. H. Levitt and R. J. Whitby, *Angew. Chem. Int. Ed.* **2019**, *58*, 5038-5043; i) M. Murata, Y. Murata and K. Komatsu, *Chem. Commun.* **2008**, 6083-6094; j) T. Sternfeld, R. E. Hoffman, M. Saunders, R. J. Cross, M. S. Syamala and M. Rabinovitz, *J. Am. Chem. Soc.* **2002**, *124*, 8786-8787.

[2] a) H. Cong, B. Yu, T. Akasaka and X. Lu, *Coord. Chem. Rev.* **2013**, *257*, 2880-2898; b) M. R. Cerón, F.-F. Li and L. A. Echegoyen, *J. Phys. Org. Chem.* **2014**, *27*, 258-264; c) A. A. Popov, S. Yang and L. Dunsch, *Chem. Rev.* **2013**, *113*, 5989-6113; d) S. Osuna, M. Swart and M. Solà, *Phys. Chem. Chem. Phys.* **2011**, *13*, 3585-3603; e) X. Lu, T. Akasaka and S. Nagase, *Chem. Commun.* **2011**, *47*, 5942-5957; f) *Endofullerenes: A New Family of Carbon Cluster*, Eds.: T. Akasaka and S. Nagase, Kluwer, Dordrecht, **2002**; g) A. Rodríguez-Fortea, A. L. Balch and J. M. Poblet, *Chem. Soc. Rev.* **2011**, *40*, 3551-3563; h) M. Yamada, T. Akasaka and S. Nagase, *Acc. Chem. Res.* **2010**, *43*, 92-102.

[3] a) J. Zhao, X. Huang, P. Jin and Z. Chen, *Coord. Chem. Rev.* **2015**, *289-290*, 315-340; b) M. N. Chaur, F. Melin, A. L. Ortiz and L. Echegoyen, *Angew. Chem. Int. Ed.* **2009**, *48*, 7514-7538; c) D. M. McCluskey, T. N. Smith, P. K. Madasu, C. E. Coumbe, M. A. Mackey, P. A. Fulmer, J. H. Wynne, S. Stevenson and J. P. Phillips, *ACS Appl. Mater. Interfaces* **2009**, *1*, 882-887; d) S. Osuna, M. Swart and M. Solà, *Chem. Eur. J.* **2010**, *16*, 3207-3214; e) M. Izquierdo, B. Platzer, A. J. Stasyuk, O. A. Stasyuk, A. A. Voityuk, S. Cuesta, M. Solà, D. M. Guldi and N. Martín, *Angew. Chem. Int. Ed.* **2019**, *58*, 6932-6937; f) J. D. Wilson, W. C. Broaddus, H. C. Dorn, P. P. Fatouros, C. E. Chalfant and M. D. Shultz, *Bioconjugate Chem.* **2012**, *23*, 1873-1880; g) D. M. Guldi, B. M. Illescas, C. M. Atienza, M. Wielopolski and N. Martin, *Chem. Soc. Rev.* **2009**, *38*, 1587-1597; h) P. Anilkumar, F. Lu, L. Cao, P. G. Luo, J. H. Liu, S. Sahu, I. K. N. Tackett, Y. Wang and Y. P. Sun, *Curr. Med. Chem.* **2011**, *18*, 2045-2059.

[4] a) X. Lu, L. Bao, T. Akasaka and S. Nagase, *Chem. Commun.* **2014**, *50*, 14701-14715; b) A. Mateo-Alonso, D. Bonifazi and M. Prato in *Chapter 7 - Functionalization and applications of [60]fullerene*, (Ed. L. Dai), Elsevier, Amsterdam, **2006**, pp. 155-189; c) A. Hirsch, *Angew. Chem. Int. Ed. Engl.* **1993**, *32*, 1138-1141; d) R. Taylor and D. R. Walton, *Nature* **1993**, *363*, 685-693; e) A. Hirsch and M. Brettreich, *Fullerenes: Chemistry and Reactions*, John Wiley & Sons, Weinheim, **2004**; f) M. Chen, X. Lu, M. R. Cerón, M. Izquierdo and L. Echegoyen in *Chemistry of Conventional Endohedral Metallofullerenes and Cluster Endohedral Fullerenes*, Eds.: X. Lu, L. Echegoyen, A. L. Balch, S. Nagase and T. Akasaka, CRC Press, Boca Ratón, **2014**, pp. 173-210.

[5] T. Suzuki, Q. Li, K. C. Khemani, F. Wudl and Ö. Almarsson, *Science* **1991**, *254*, 1186-1188.

[6] a) M. Prato and M. Maggini, *Acc. Chem. Res.* **1998**, *31*, 519–526; b) F. Diederich, L. Isaacs and D. Philp, *Chem. Soc. Rev.* **1994**, *23*, 243-255; c) C. Thilgen and F. Diederich, *Chem. Rev.* **2006**, *106*, 5049-5135; d) W.-B. Ko and K.-N. Baek, *Phys. Solid State* **2002**, *44*, 424-426; e) J. Gao, Y. Wang, K. M. Folta, V. Krishna, W. Bai, P. Indeglia, A. Georgieva, H. Nakamura, B. Koopman and B. Moudgil, *PLOS ONE* **2011**, *6*, e19976; f) M. D. Tzirakis and M. Orfanopoulos, *Chem. Rev.* **2013**, *113*, 5262-5321.

[7] a) W. Śliwa, *Fullerene Sci. Techn.* **1997**, *5*, 1133-1175; b) B. Kräutler and J. Maynollo, *Tetrahedron* **1996**, *52*, 5033-5042.

[8] M. Prato, V. Lucchini, M. Maggini, E. Stimpfl, G. Scorrano, M. Eiermann, T. Suzuki and F. Wudl, *J. Am. Chem. Soc.* **1993**, *115*, 8479-8480.

[9] C. Bingel, *Chem. Ber.* **1993**, *126*, 1957-1959.

[10] H. W. Kroto, *Nature* **1987**, *329*, 529-531.

[11] R. D. Bolskar, A. F. Benedetto, L. O. Husebo, R. E. Price, E. F. Jackson, S. Wallace, L. J. Wilson and J. M. Alford, *J. Am. Chem. Soc.* **2003**, *125*, 5471-5478.

[12] a) C. M. Cardona, A. Kitaygorodskiy and L. Echegoyen, *J. Am. Chem. Soc.* **2005**, *127*, 10448-10453; b) C. M. Cardona, B. Elliott and L. Echegoyen, *J. Am. Chem. Soc.* **2006**, *128*, 6480-6485.

[13] Y. Hu, A. Solé-Daura, Y.-R. Yao, X. Liu, S. Liu, A. Yu, P. Peng, J. M. Poblet, A. Rodríguez-Fortea, L. Echegoyen and F.-F. Li, *Chem. Eur. J.* **2020**, *26*, 1748-1753.

[14] a) M. N. Chaur, F. Melin, A. J. Athans, B. Elliott, K. Walker, B. C. Holloway and L. Echegoyen, *Chem. Commun.* **2008**, 2665-2667; b) N. Alegret, M. N. Chaur, E. Santos, A. Rodriguez-Fortea, L. Echegoyen and J. M. Poblet, *J. Org. Chem.* **2010**, 8299–8302.

[15] T. Cai, C. Slebodnick, L. Xu, K. Harich, T. E. Glass, C. Chancellor, J. C. Fettinger, M. M. Olmstead, A. L. Balch, H. W. Gibson and H. C. Dorn, *J. Am. Chem. Soc.* **2006**, *128*, 6486-6492.

[16] a) S. Aoyagi, Y. Sado, E. Nishibori, H. Sawa, H. Okada, H. Tobita, Y. Kasama, R. Kitaura and H. Shinohara, *Angew. Chem. Int. Ed.* **2012**, *51*, 3377-3381; b) S. Fukuzumi, K. Ohkubo, Y. Kawashima, D. S. Kim, J. S. Park, A. Jana, V. M. Lynch, D. Kim and J. L. Sessler, *J. Am. Chem. Soc.* **2011**, *133*, 15938-15941; c) H. Ueno, K. Kokubo, Y. Nakamura, K. Ohkubo, N. Ikuma, H. Moriyama, S. Fukuzumi and T. Oshima, *Chem. Commun.* **2013**, *49*, 7376-7378.

[17] a) H. Kawakami, H. Okada and Y. Matsuo, *Organic Letters* **2013**, *15*, 4466-4469; b) H. Ueno, H. Kawakami, K. Nakagawa, H. Okada, N. Ikuma, S. Aoyagi, K. Kokubo, Y. Matsuo and T. Oshima, *J. Am. Chem. Soc.* **2014**, *136*, 11162-11167.

[18] Y. García-Rodeja, M. Solà, F. M. Bickelhaupt and I. Fernández, *Chem. Eur. J.* **2017**, *23*, 11030-11036.

[19] a) M. Garcia-Borràs, M. R. Cerón, S. Osuna, M. Izquierdo, J. M. Luis, L. Echegoyen and M. Solà, *Angew. Chem. Int. Ed.* **2016**, *55*, 2374-2377; b) J. P. Martínez, M. Garcia-Borràs, S. Osuna, J. Poater, F. M. Bickelhaupt and M. Solà, *Chem. Eur. J.* **2016**, *22*, 5953-5962; c) Y. N. Biglova, I. M. Sakhautdinov, R. N. Garifullin, G. F. Sakhautdinova and A. G. Mustafin, *New J. Chem.* **2020**, *44*, 7277-7285; d) N. M. Thong, T. C. Ngo, D. Q. Dao, T. Duong, Q. T. Tran and P. C. Nam, *J. Mol. Model.* **2016**, *22*, 113; e) N. Alegret, A. Rodríguez-Fortea and J. M. Poblet, *Chem. Eur. J.* **2013**, *19*, 5061-5069; f) N. Alegret, P. Salvadó, A. Rodríguez-Fortea and J. M. Poblet, *J. Org. Chem.* **2013**, *78*, 9986-9990.

[20] S. Osuna, M. Swart and M. Solà, *J. Phys. Chem. A* **2011**, *115*, 3491-3496.

[21] a) L. Feng, T. Nakahodo, T. Wakahara, T. Tsuchiya, Y. Maeda, T. Akasaka, T. Kato, E. Horn, K. Yoza, N. Mizorogi and S. Nagase, *J. Am. Chem. Soc.* **2005**, *127*, 17136–17137; b) L. Feng, T. Tsuchiya, T. Wakahara, T. Nakahodo, Q. Piao, Yutaka Maeda, T. Akasaka, T. Kato, K. Yoza, E. Horn, N. Mizorogi and S. Nagase, *J. Am. Chem. Soc.* **2006**, *128*, 5990–5991; c) L. Feng, T. Wakahara, T. Nakahodo, T. Tsuchiya, Q. Piao, Y. Maeda, Y. Lian, T. Akasaka, E. Horn, K. Yoza, T. Kato, N. Mizorogi and S. Nagase, *Chem. Eur. J.* **2006**, *12*, 5578-5586.

[22] A. V. Marenich, C. J. Cramer and D. G. Truhlar, *J. Phys. Chem. B* **2009**, *113*, 6378-6396.

[23] M. J. Frisch, G. W. Trucks, H. B. Schlegel, G. E. Scuseria, M. A. Robb, J. R. Cheeseman, G. Scalmani, V. Barone, G. A. Petersson, H. Nakatsuji, X. Li, M. Caricato, A. V. Marenich, J. Bloino, B. G. Janesko, R. Gomperts, B. Mennucci, H. P. Hratchian, J. V. Ortiz, A. F. Izmaylov, J. L. Sonnenberg, Williams, F. Ding, F. Lipparini, F. Egidi, J. Goings, B. Peng, A. Petrone, T. Henderson, D. Ranasinghe, V. G. Zakrzewski, J. Gao, N. Rega, G. Zheng, W. Liang, M. Hada, M. Ehara, K. Toyota, R. Fukuda, J. Hasegawa, M. Ishida, T. Nakajima, Y. Honda, O. Kitao, H. Nakai, T. Vreven, K. Throssell, J. A. Montgomery Jr., J. E. Peralta, F. Ogliaro, M. J. Bearpark, J. J. Heyd, E. N. Brothers, K. N. Kudin, V. N. Staroverov, T. A. Keith, R. Kobayashi, J. Normand, K. Raghavachari, A. P. Rendell, J. C. Burant, S. S. Iyengar, J. Tomasi, M. Cossi, J. M. Millam, M. Klene, C. Adamo, R. Cammi, J. W. Ochterski, R. L. Martin, K. Morokuma, O. Farkas, J. B. Foresman and D. J. Fox in *Gaussian 16 Rev. C.01*, *Vol.* Wallingford, CT, **2016**.

[24] a) A. D. Becke, *J. Chem. Phys.* **1993**, *98*, 5648-5652; b) C. Lee, W. Yang and R. G. Parr, *Phys. Rev. B* **1988**, *37*, 785-789.

[25] a) S. Grimme, J. Antony, S. Ehrlich and H. Krieg, *J. Chem. Phys.* **2010**, *132*, 154104; b) S. Grimme, S. Ehrlich and L. Goerigk, *J. Comput. Chem.* **2011**, *32*, 1456-1465; c) S. Grimme, A. Hansen, J. G. Brandenburg and C. Bannwarth, *Chem. Rev.* **2016**, *116*, 5105-5154.
[26] A. D. Becke and E. R. Johnson, *J. Chem. Phys.* **2007**, *127*, 154108.
[27] A. Schäfer, H. Horn and R. Ahlrichs, *J. Chem. Phys.* **1992**, *97*, 2571-2577.
[28] S. Osuna, J. Morera, M. Cases, K. Morokuma and M. Solà, *J. Phys. Chem. A* **2009**, *113*, 9721–9726.
[29] a) K. Fukui, *J. Phys. Chem.* **1970**, *74*, 4161-4163; b) C. Gonzalez and H. B. Schlegel, *J. Chem. Phys.* **1989**, *90*, 2154-2161.
[30] A. Schäfer, C. Huber and R. Ahlrichs, *J. Chem. Phys.* **1994**, *100*, 5829-5835.

Entry for the Table of Contents

Insert graphic for Table of Contents here.

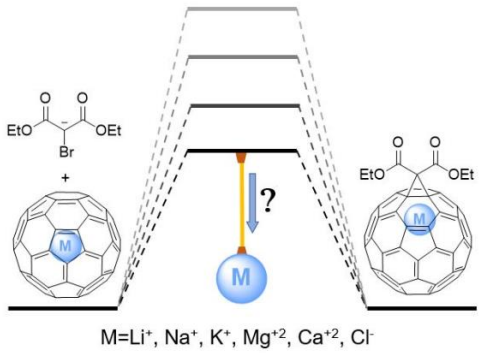

Insert text for Table of Contents here.

Similar to the Diels-Alder (DA) cycloaddition, the Bingel-Hirsch (BH) addition of bromomalonate to C_{60} is accelerated by the presence of monocations (Li^+, Na^+, K^+) encapsulated in the fullerene. However, at variance with the DA cycloaddition, the performance of the BH deteriorates when changing the monocations by dications (Mg^{+2}, Ca^{+2}) due to the increase of the energy barriers in the last step of the BH addition.

Institute and/or researcher Twitter usernames: @dimocat_iqcc @iqccUdG @udgrecerca @paubesalu @josepmluis @miquelsola